CORA Cork Open Research Archive
Cartlann Taighde Oscailte Chorcaí

Title	Time- and intensity-dependent broadband cavity-enhanced absorption spectroscopy with pulsed intra-cavity laser-induced plasmas
Authors	Keary, Bryan P.;Ruth, Albert A.
Publication date	2019-12-04
Original Citation	Keary, Bryan P.; Ruth, Albert A. (2019) 'Time- and intensity-dependent broadband cavity-enhanced absorption spectroscopy with pulsed intra-cavity laser-induced plasmas'. Optics Express, 27(25), pp. 36864-36874. doi: 10.1364/OE.27.036864
Type of publication	Article (peer-reviewed)
Link to publisher's version	http://www.opticsexpress.org/abstract.cfm?URI=oe-27-25-36864 - 10.1364/OE.27.036864
Rights	© 2019 Optical Society of America under the terms of the OSA Open Access Publishing Agreement - https://www.osapublishing.org/library/license_v1.cfm#VOR-OA
Download date	2026-09-12 16:50:08
Item downloaded from	https://hdl.handle.net/10468/9347

UCC
University College Cork, Ireland
Coláiste na hOllscoile Corcaigh

Research Article | Vol. 27, No. 25 / 9 December 2019 / Optics Express 36864

Optics EXPRESS

Time- and intensity-dependent broadband cavity-enhanced absorption spectroscopy with pulsed intra-cavity laser-induced plasmas

BRYAN P. KEARY AND ALBERT A. RUTH*,

Department of Physics & Environmental Research Institute, University College Cork, Cork, Ireland
a.ruth@ucc.ie

Abstract: A pulsed laser-induced plasma (LIP) was generated in ambient air inside a high-finesse ($F \approx 5200$) *near-concentric* optical cavity. The optical plasma emission was successfully trapped and sustained by the cavity, manifested by ring-down times in excess of 4 μs indicating effective mirror reflectivities of ~0.9994. The light leaking from the cavity was used to measure broadband absorption spectra of gaseous azulene under ambient air conditions between 580 and 645 nm, employing (i) intensity-dependent cavity-enhanced, and (ii) time-dependent cavity-ring down methodologies. Minimum detectable absorption coefficients of 4.7×10^{-8} cm^{-1} and 7.4×10^{-8} cm^{-1} were achieved for the respective approaches. The two approaches were compared and implications of pulsed excitation for gated intensity-dependent measurements were discussed.

© 2019 Optical Society of America under the terms of the OSA Open Access Publishing Agreement

1. Introduction

The use of laser-induced plasmas (LIP) in air as intra-cavity light sources for incoherent broadband cavity-enhanced absorption spectroscopy (IBBCEAS) [1] was first demonstrated by Ruth et al. in 2015 [2]. Placing the incoherent light generation inside a high-finesse optical cavity in the form of an LIP was motivated by the objective of finding a way of increasing the overall amount of incoherent light inside the cavity, and thus improving the generally low coupling efficiency of incoherent light to optically stable cavities; a fundamental limitation of IBBCEAS. A difficulty with this approach to CEAS is that an LIP in a cavity constitutes an inherent time-dependent optical loss, until the carrier gas, in which the plasma is generated, has returned to an equilibrium state. The corresponding time is substantially longer than the light round trip time in the cavity and successfully sustaining the light in the cavity was seen as the main initial challenge in [2]. The experimental parameters to generate the intra-cavity plasma in [2] were thus chosen to minimise the physical dimensions of the plasma. Hence the LIPs were generated with relatively small pulse energies of ~ 2.6 mJ and high peak powers of ~ 13 GW, using a (200 fs) Nd:Glass laser. The pulses were focused into the centre of a *confocal* high-finesse optical cavity (length 40 cm) to maximize the light collection efficiency of light leaking from the cavity. This approach generated short-lived and spatially small plasmas, at the expense of plasma brightness. Nevertheless, despite the optical losses posed by the LIP, the optical emission from the plasma was sustained by the cavity under the described conditions and used to measure IBBCEAS spectra of static gaseous azulene in ambient air (560 – 650 nm), and of molecular oxygen (625 – 635 nm).

The signal-to-noise ratio (SNR) in this approach to IBBCEAS was limited by the overall low brightness of the LIP, thus necessitating relatively long integration times and substantial signal amplification. In contrast to [2], in this study we generated the LIPs by way of a pulsed *nanosecond* Nd:YAG laser in a cavity with a *near-concentric* geometry. The laser provided pulses of ~ 10 ns duration with higher pulse energy (~ 55 mJ) but lower peak power (5.5 MW), resulting in a larger plasma plume with greatly increased brightness. It will be shown that, despite the expected higher optical losses of the LIP, light was well sustained in the near-concentric cavity and the SNR of IBBCEAS measurements was improved in comparison to [2].

#379453 https://doi.org/10.1364/OE.27.036864
Journal © 2019 Received 1 Oct 2019; revised 9 Nov 2019; accepted 19 Nov 2019; published 4 Dec 2019

Optics EXPRESS

In addition to intensity-dependent IBBCEAS measurements, the time-dependence of the spectrum of light leaking from the cavity was also monitored to investigate the viability of broadband cavity ring-down (CRD) spectra obtained with the LIP-based approach for quantitative analysis of the obtained spectra [3]. Absolute absorption measurements with IBBCEAS require the wavelength-dependent mirror reflectivity, $R(\lambda)$, to be known. In CEAS, mirror reflectivities are typically determined by measuring the optical loss from a known concentration of an absorbing species [4,5], or via the known Rayleigh scattering cross-sections of two gases [6,7]. In this study we demonstrate how the pulsed nature of the LIP provides an *in situ* calibration of the effective reflectivity of the cavity mirrors based on the broadband ring-down time measurement of the plasma emission within the cavity (also cf. [8]). In this context, it is important to note that the wavelength-dependent emission from the LIP does not exclusively possess a plain thermal continuum spectrum (which exclusively depends on the temperature of the plasma), but also contains superimposed time-dependent atomic emission lines due to the recombination of electrons during plasma expansion. These plasma recombination dynamics cause the time-dependence of the emission intensity to be inherently wavelength-dependent during the plasma lifetime. The influence of these characteristic emissions on the initial conditions for sustaining light inside the cavity across the low loss wavelength range of the mirrors and its consequence for absorption measurements will be outlined and discussed in this publication.

In Section 2 details of the experimental setup are provided, and in Section 3 absorption spectra of gaseous azulene measured with LIP-based CRDS and IBBCEAS are presented; pros and cons are discussed also in conjunction with aspects concerning mirror reflectivity calibration.

2. Experimental setup

A schematic of the experimental setup is shown in Fig. 1. The laser-induced plasma was generated with an actively Q-switched Nd:YAG laser (Lumonics HY400), which delivered pulses with an energy of ~ 55 mJ at a repetition rate of 9.7 Hz, with a pulse duration (FWHM) of ~ 10 ns. The emission of the laser resonator at 1064 nm was frequency doubled (with a thermalised KDP crystal), and both the fundamental wavelength (1064 nm) as well as the second harmonic (532 nm) were present in the output light. For plasma generation the laser pulses were focused to the centre of an optical cavity using a lens of 3 cm focal length (L_1, see Fig. 1). The maximum power density on the optical axis of the cavity was estimated to be approximately 10^{11} W cm^{-2} assuming a beam waist of ~ 30 µm at the focus of L_1.

The optical cavity was formed by two high reflectivity (HR) mirrors (Layertec GmbH) which had a diameter of 4 cm and a radius of curvature of 40 cm, with a nominal on-axis reflectivity of $R > 0.9997$ over the spectral range 580 – 635 nm (values according to manufacturer's data sheet). The mirror separation was $L = 79.3 \pm 0.1$ cm, giving the cavity a *near-concentric* geometry; the space between the mirrors was partially enclosed but essentially open to ambient lab air. The light leaking from one of the cavity mirrors was spectrally filtered with a notch filter at 532 nm and imaged with an achromatic lens onto the aperture of a circular-to-rectangular fibre bundle, which guided the light to the entrance slit of a polychromator/iCCD assembly (Shamrock 303i / Andor iStar DH740_18mm). The light detection assembly was used to spectrally and temporally monitor the plasma emission leaking from the cavity. The dispersive polychromator contained a blazed grating with 600 lines/mm. In conjunction with an entrance slit width of 100 µm (which corresponded to the diameter of individual strands in the fibre bundle) the resolution was determined to be ≈ 0.34 nm in the spectral range from 560 – 650 nm using a low pressure neon Pen-Ray lamp.

For absorption measurements, gaseous azulene was introduced into the setup by sublimation of molecular azulene crystals in the open cavity at room temperature, and lowering its concentration subsequently by flushing the cavity with dry compressed air for ca. 10 min [2].

Optics EXPRESS

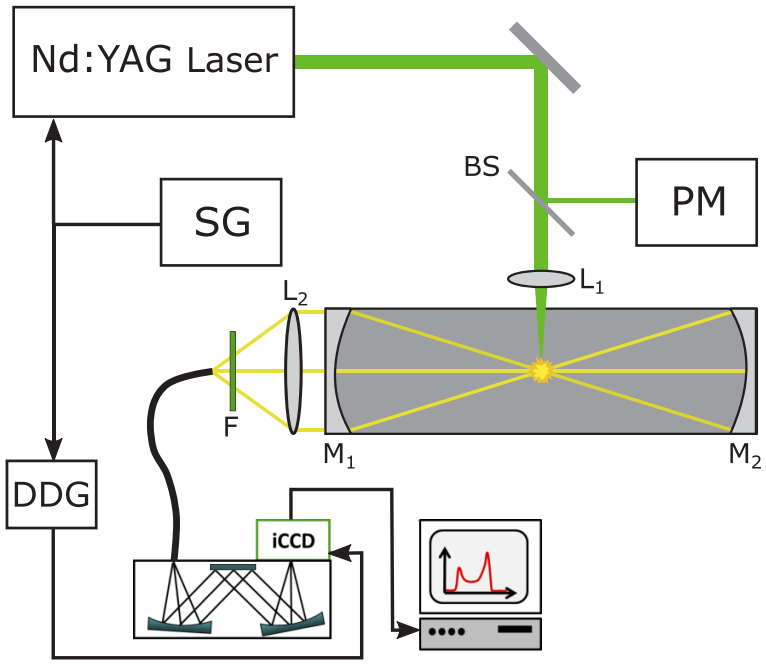

Fig. 1. Schematic of the experimental setup. The Nd:YAG laser produced 10 ns pulses with an energy of ~ 55 mJ. L_1 (f = 3 cm): Focusing lens for plasma generation. L_2 (f = 12 cm): Achromatic lens to image light leaking from the cavity to a light guide (fibre bundle). F: notch filter (FWHM = 17 nm) centered at 532 nm. $M_{1,2}$: High reflectivity ($R \sim 0.9993$, cf. Section 3) plano-concave ($r = -40$ cm) dielectric cavity mirrors centered at 610 nm. BS: 95/5 beamsplitter. PM: Power meter. SG: Signal generator (output 9.7 Hz) providing laser trigger and signal for digital delay generator (DDG) of the iCCD.

3. Results and discussion

Figure 2 shows the measured *near-concentric* cavity output intensity from 0 to 13 µs after plasma formation, measured in steps of 500 ns, accumulated over 500 individual plasma excitations per step, with a measurement gate width of 500 ns (corresponding total integration time of 250 µs per step). Considering that a high power ns-pulse was used for plasma formation, and the associated substantial physical dimension of the plasma (~ 3 – 4 mm diameter), the intensity level at which light was sustained in the cavity was surprisingly high in comparison to prior work [2]. The time-dependence in Fig. 2 shows that light is indeed sustained within the cavity by more than 12 µs, i.e. sufficiently long to allow cavity-based absorption measurements. As expected, a significant initial optical loss due to the plasma formation in the cavity decreases the output intensity immediately after laser excitation by a factor of ~ 7. This substantial intensity decrease lasts for approximately ~ 1.5 µs. Thereafter, the cavity output intensity begins to decay mono-exponentially (ring-down). The transition from the initially strong loss to mono-exponential behaviour is further discussed in Section 3.1. This behaviour is in contrast to the time-dependence observed in the case of a *confocal* cavity geometry (see [2]), where an intensity maximum was observed during the time dependence of the light leaking from the cavity. The most probable reasons for this difference is a non-linear refractive index change during plasma recombination in conjunction with a finite aperture size in the light collection [9,10].

The time interval over which the light intensity leaking from the cavity decays mono-exponentially can be used for CRDS as well as IBBCEAS measurements. Before both approaches

Optics EXPRESS

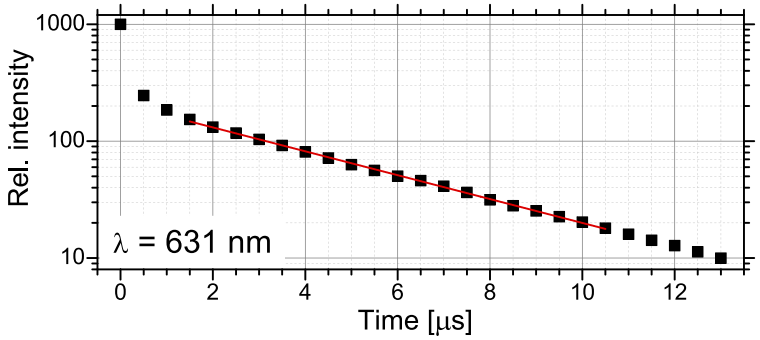

Fig. 2. Relative cavity output intensity for a laser-induced plasma at the centre of a 79.3 cm cavity, measured at λ = 631 nm. The cavity output intensity was accumulated over 500 plasma pulses with a gate duration of 500 ns, giving a total integration time of 250 µs for each data point. After the initial decrease in intensity by a factor of ~ 7, mono-exponential decay behaviour is observed after approximately 1.5 µs. Corresponding ring-down time: 4.24 µs. Red trace: Linear regression fit to data points shown.

are discussed and compared based on gaseous azulene absorption measurements (Section 3.2), the procedure to measure the effective mirror reflectivity will be outlined.

3.1. Effective reflectivity calibration

The pulsed nature of the LIP facilitates the *in situ* calibration of the effective mirror reflectivity, $R(\lambda)$, in air at ~ 1 atm, based on the wavelength-dependent ring-down time, $\tau(\lambda)$. Without a sample species present in the cavity, the ring-down time was determined from the time dependence of the light leaking from an (air-filled) cavity in the time window from 1.5 to 10.5 µs after plasma formation, measured in steps of 0.5 µs. This measurement, without azulene in the cavity, corresponds to the spectrum of $\tau_0(\lambda)$ in Section 3.2.1. The wavelength-dependent reflectivity, $R(\lambda) = 1 - \{L/[c\,\tau_0(\lambda)]\}$, where c is the speed of light, is shown in Fig. 3 (left axis) along with the corresponding ring-down time (right axis). It should be noted that, depending on the carrier gas used for plasma formation (air in the current case), reflectivities determined in this way are affected by long-lived recombination emissions from the plasma. In the present case long lived emissions are observed around 616 nm and beyond 642 nm, where apparently longer lifetimes are observed (see Fig. 3). Around the spectral positions where recombination lines are located a mono-exponential fit function (as used in this analysis) is inadequate for the description of the time-dependence of the intensity. The deviation from the truly mono-exponential behaviour leads to the observed structure in the spectrum around 616 nm and beyond 642 nm. Transition rates of plasma recombination processes, however, could not be deduced from this approach in a straightforward manner. As the reflectivity is expectedly a smooth function of the wavelength over the high reflectivity range of the mirrors, emission lines can be readily eliminated by appropriately modelling the data with a polynomial fit, B-splines, or usage of Fourier filters; (see red trace in Fig. 3). The long-lived plasma emissions should ideally be identified and studied for specific carrier gases and experimental scenarios before executing absorption measurements. Finally it should be noted that the maximum reflectivity of $R \approx 0.9994$ at ~ 640 nm is lower than the quoted nominal on-axis reflectivity of the manufacturer, because this method yields merely an effective reflectivity. High order TEM modes are populated by this approach as the entire mirror surface is used to sustain light in the cavity. The reflectivity is based on an effective mean over all relevant mode lifetimes (applicable over the entire mirror surface) for a given cavity geometry.

This *in situ* reflectivity calibration provides a simple means of measuring absolute extinction coefficients with this approach to IBBCEAS.

Optics EXPRESS

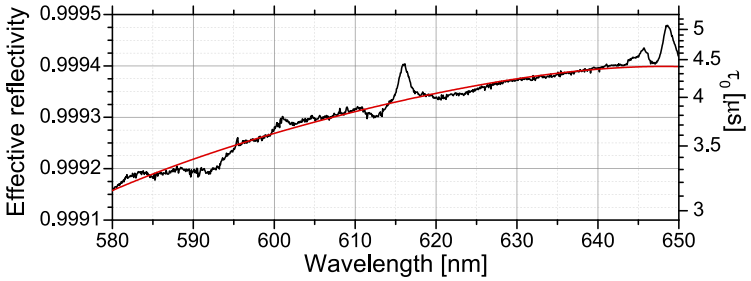

Fig. 3. Black race: Effective mirror reflectivity (left-axis) calculated from the wavelength-dependent ring-down time of light leaking from the cavity (right-axis). Red trace: Fourth-order polynomial fit to the measured reflectivity spectrum.

3.2. Absorption measurements

3.2.1. Broadband CRDS

The weak symmetry forbidden $S_1 \leftarrow S_0$ transition in azulene has been used extensively as a test case for cavity-enhanced absorption methods [1,11]. Figure 4 shows the ro-vibronic contour bands of the $S_1 \leftarrow S_0$ absorption spectrum of gaseous azulene ($C_{10}H_8$) in ambient air measured

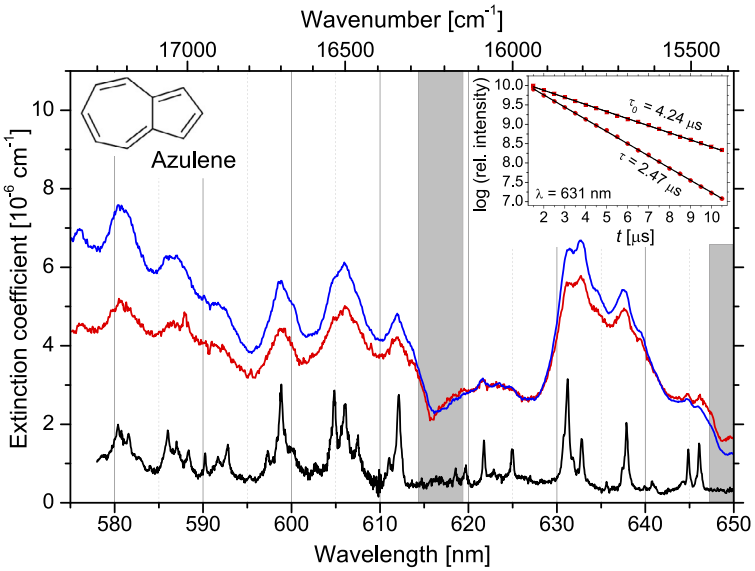

Fig. 4. Red trace: Broadband CRDS spectrum of azulene obtained from the ring-down time of light leaking from the cavity between 1.5 and 10.5 μs after plasma formation. The ring-down time was measured in steps of 0.5 μs accumulated over 500 plasma pulses (integration time of 250 μs) per step. Blue trace: IBBCEAS spectrum of azulene obtained by accumulating the cavity output for 500 plasma pulses from 1.5 to 10.5 μs after plasma formation (gated data acquisition); total integration time of 4.5 ms. Determination of the extinction coefficient is based on the effective reflectivity shown in Fig. 3. Black trace: Arbitrarily scaled cavity ring-down absorption spectrum of jet-cooled azulene from [12] for comparison. Inset: Semi-logarithmic plot of the cavity output intensity showing the ring-down time measurements including the respective fit without and with azulene present in the cavity (red squares and dots respectively), measured at 631 nm (also compare Fig. 2).

Optics EXPRESS

with different experimental approaches. The contour bands represent only part of the azulene spectrum at excess energies between ~ 1100 cm^{-1} and ~ 3100 cm^{-1} above the 0 – 0 transition, which is located at 14283 cm^{-1} [12].

The red trace in Fig. 4 is the CRDS spectrum and was determined from the wavelength-dependent ring-down time of the plasma emission within the cavity. The ring-down times were calculated based on the cavity output intensity measured in steps of 0.5 µs from 1.5 to 10.5 µs after plasma formation. Each step was accumulated over 500 plasma pulses, giving a total integration time of 250 µs per step. This yielded an average SNR of 51 across the spectral range, with the noise level defined as the 2σ noise in the absorption background determined from two separate CRD measurements without azulene present within the cavity. This SNR corresponded to a minimum detectable absorption coefficient, ε_{min}, of 7.4×10^{-8} cm^{-1}.

This stepwise approach to broadband CRDS resulted in an overall measurement time of ~ 16 min. For comparison, the cavity ring-down absorption spectrum of *jet-cooled* azulene (black trace) from a previous study [12] is also shown in Fig. 4. Apart from the narrower band structure of the jet-cooled azulene spectrum, which is caused by the significantly lower temperature in the collisionless regime, and the higher resolution of the corresponding jet measurement, the general agreement between the two spectra is satisfactory. The steadily increasing absorption background towards shorter wavelengths in the CRDS spectrum in Fig. 4, is due to overlapping absorption features resulting from an increased density of states at higher energies in combination with the lower spectral resolution of this measurement. A discussion of the background in the absorption spectrum can also be found in Ruth et al. [11,12].

3.2.2. IBBCEAS

The IBBCEA spectrum (blue trace) shown in Fig. 4 was obtained from an accumulation of the cavity output following 500 LIP excitations. The emission was gated between 1.5 and 10.5 µs after plasma formation, giving a total integration time of 4.5 ms. With a laser repetition rate of 9.7 Hz this corresponds to a total measurement time of ~ 52 s. This overall measurement time is ~ 18 times shorter than that for the CRD measurement and yields an SNR of the IBBCEA spectrum of 104, which is a factor of ~ 2 larger than that of the CRD spectrum. As before, the SNR was calculated from the 2σ noise in the absorption baseline which was determined from two separate accumulations of the cavity output without azulene present (i.e. $I_0/I_0 - 1$). The SNR of 104 corresponds to a minimum extinction coefficient of $\varepsilon_{min} = 4.7 \times 10^{-8}$ cm^{-1}. Extinction coefficients were determined using the effective reflectivity curve outlined in Section 3.1. However, due to the significant uncertainty in the absolute azulene concentration (which is caused by the rather basic introduction of gaseous azulene into the cavity under ambient conditions) deducing absorption cross-sections from this measurement was not attempted.

The IBBCEA spectrum (blue solid trace), which is based on a pulsed and *gated* intensity measurement, shows good qualitative agreement with the spectrum measured with the CRDS approach (red solid trace). However, the extinction coefficients measured via IBBCEAS appear to be systematically larger than those measured with CRDS, by roughly a factor of 1.5 (Fig. 4). Even though this difference could be due to a different number density of azulene in the two measurements, there is also indeed a generic reason for the observed discrepancy: The IBBCEAS measurement is pulsed and gated, and the data acquisition window is delayed by a time required for plasma equilibration and recombination (in the present case ~ 1.5 µs). During plasma equilibration the pre-conditions for Lambert-Beer absorption are not fulfilled and the cavity output does not decay mono-exponentially. The necessary delay for the measurement causes the IBBCEAS signal to be systematically overestimated; a way to account for this experimental bias in general will be discussed next.

In IBBCEAS the fractional absorption $I_0/I-1$ is determined, which is based on the measurement of the time-integrated intensities without the sample, I_0, and with the sample, I, in the cavity. The

Optics EXPRESS

measurement conditions for determining I and I_0 must (ideally) be identical for the measurement principle to hold [1,13]. Introducing a delay in a pulsed IBBCEAS measurement scheme impinges on this condition, since absorption already takes place during the delay before the start time of the data acquisition, when a sample is present in the cavity (a schematic of the situation is shown in Fig. 5). Thus the intensities, A_{I_0} and A_I (see Fig. 5), at the time, t_{start}, when signal integration begins, are not identical; in fact $A_{I_0} > A_I$. The *measured absorption* is therefore larger than the *true absorption* by an amount that corresponds to the absorption of light in the cavity during the delay time (between $t = 0$ s and t_{start}). As a consequence pulsed IBBCEA spectra measured with a delay tend to exhibit larger absorptions than CRD spectra, which are not affected by the delay, due to the intensity independent measurement principle. It should be noted that this source of error is not unique to using laser-induced plasmas, but applies to all *pulsed* IBBCEAS systems where a delay after light generation is necessary for whatever experimental reason. The shorter the delay, the smaller the discrepancy between the measured and the true absorption spectrum. It should be noted that IBBCEAS has the advantage of measurement times being shorter due to using only one long gate window in comparison of the CRDS approach, where the scanning of the delay of the gate window is significantly more cumbersome; hence higher signal to noise ratios can be achieved using IBBCEAS.

Accounting for the absorption offset analytically is not possible. Thus we tried to correct the gated IBBCEA spectra using two similar numerical procedures, which are outlined and compared here. The approach is illustrated in Fig. 5, where typical schematic decays after pulsed excitation are shown for the cases without and with the sample (upper and lower panel, respectively). The assumptions (AS*i*) are made that, at each wavelength in the relevant spectral range, the following quantities are known in a typical IBBCEA measurement:

(AS1) The value of the *time-integrated signal* with and without a sample in the cavity (dark grey areas in Fig. 5, denoted I and I_0).

(AS2) The *ring-down times of the cavity without the sample*, τ_0, from which the mirror reflectivity, $R(\lambda)$, is deduced (as per Section 3.1). From the latter measurement also the light signal amplitude $A(\lambda, t = 0)$ (denoted $A_{t=0}$) is known.

The time integrated cavity output is given by

$$I = A_{t=0} \int_{t_{\mathrm{start}}}^{t_{\mathrm{end}}} \exp\left(-\frac{t}{\tau}\right) \mathrm{d}t = A_{t=0}\tau \left(\exp\left(-\frac{t_{\mathrm{start}}}{\tau}\right) - \exp\left(-\frac{t_{\mathrm{end}}}{\tau}\right)\right) \tag{1}$$

Since I and $A_{t=0}$ are known from measurements as assumed in (AS1) and (AS2) the only unknown in Eq. (1) is the ring-down time τ. Through a numerical solution of the transcendental Eq. (1) the value of τ can be evaluated for each wavelength. In this case, the point of intersection of $I/A\tau$ and $\exp\left(-\frac{t_{\mathrm{start}}}{\tau}\right) - \exp\left(-\frac{t_{\mathrm{end}}}{\tau}\right)$ for varying τ was found through a graphical approach.

By obtaining $\tau(\lambda)$ the spectrum of the absorption coefficient $\varepsilon(\lambda)$ can be evaluated if, in addition to (AS2), another assumption is made:

(AS3) The light signal amplitude $A_{t=0}$ (known from (AS2)) does not strongly change between measurements with and without the sample in the cavity (cf. intercept in Fig. 5); in other words, the excitation light source (averaged over appropriate data acquisition cycles) must be stable enough not to introduce an additional systematic uncertainty in the correction.

(AS3) is a generic precondition for IBBCEAS. If it is not fulfilled, an additional systematic error arises in the form of a small additional (positive or negative) offset in the correction. There are two ways to obtain the corrected absorption coefficient from $\tau(\lambda)$, which can be jointly used as a criterion to assess (AS3), and evaluate the light source instability (drifts or fluctuations) by simple comparison of the results (see below).

Optics EXPRESS

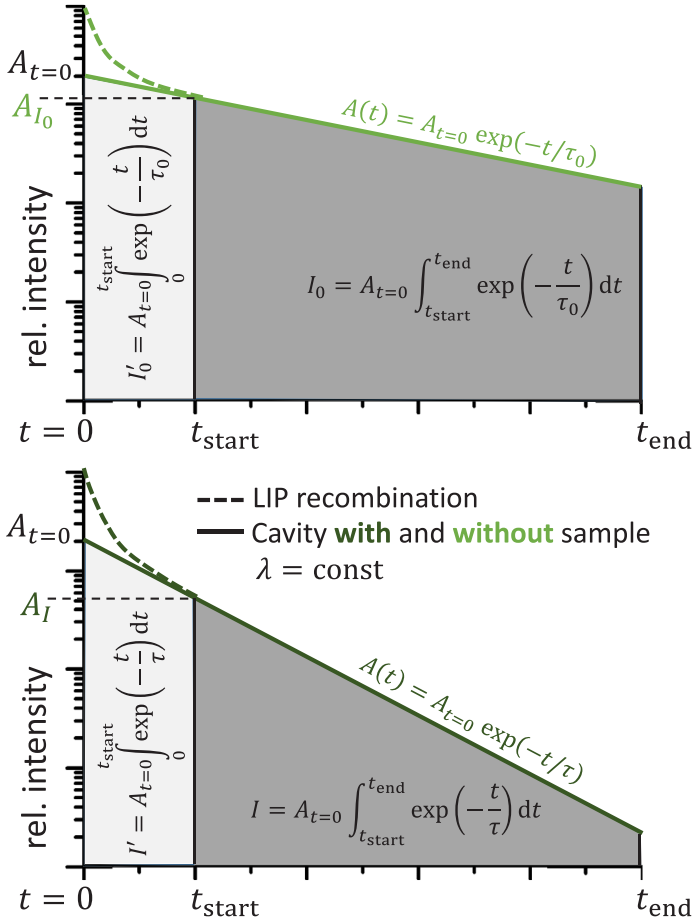

Fig. 5. Illustration of the source of error in pulsed IBBCEAS measurement with delayed (i.e. gated) data acquisition. $A(t)$ is the time-dependent cavity output intensity without (light green) and with (dark green) the sample. I and I_0 (both dark grey) are the time-integrated intensities as measured in pulsed IBBCEAS during the gate time, i.e. $(t_{end} - t_{start})$. I' and I_0' (both light grey) are the time-integrated intensities during an arbitrary delay time, t_{start}, that needs to be accounted for. If not corrected, pulsed gated IBBCEAS will deliver absorption coefficients that are too high, depending on the gate delay.

(1) *CRDS based evaluation*: As τ_0 is known from (AS2) the corrected absorption coefficient at each wavelength can be simply evaluated from

$$\varepsilon_{(1)}(\lambda) = \frac{1}{c}\left(\frac{1}{\tau(\lambda)} - \frac{1}{\tau_0(\lambda)}\right). \tag{2}$$

(2) *CEAS based evaluation*: From the numerically determined τ and $A_{t=0}$ (from (AS3)) a ring-down transient, $A(t) = A_{t=0}\exp(-t/\tau)$, can be modelled and integrated up to the delay time t_{start}, yielding the unknown contribution to the absorption signal I' (see Fig. 5). From $I_0{}'$ (known from (AS2)) and I', the new corrected IBBCEAS spectra can be determined:

$$\varepsilon_{(2)}(\lambda) = \frac{1 - R(\lambda)}{L}\left(\frac{I_0(\lambda) + I_0{}'(\lambda)}{I(\lambda) + I'(\lambda)} - 1\right) \tag{3}$$

Optics EXPRESS

The IBBCEAS data (blue trace) in Fig. 4 were corrected using Eqs. (1), (2) and (3), and are shown in comparison with the CRDS spectrum (red) in Fig. 6. Based on the complete equilibration time of the plasma in the corresponding experiment (including expansion and full ion recombination), t_{start}=1.5 µs was used for this calculation. Furthermore t_{end} = 10.5 µs based on the IBBCEAS acquisition gate window $\Delta t_{gate} = t_{end} - t_{start}$ of 9 µs, and $A_{t=0}$ from back extrapolation of the data in Fig. 2, were used at each wavelength in the spectrum.

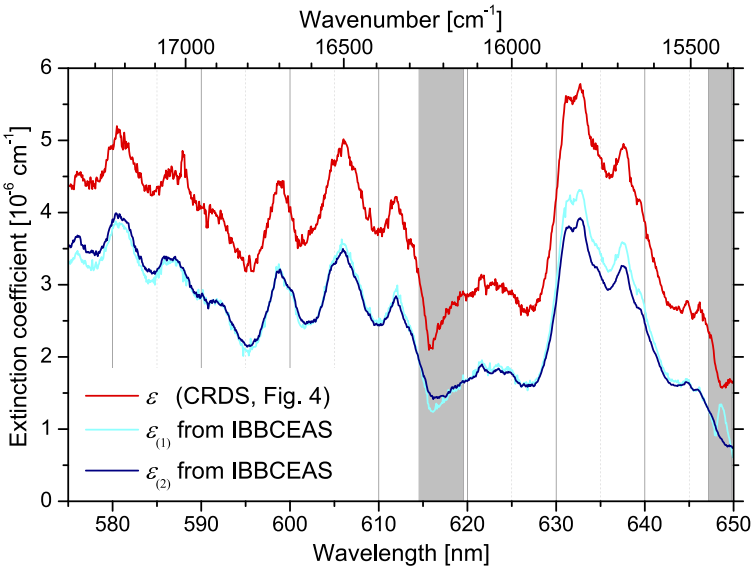

Fig. 6. Red trace: Broadband CRDS spectrum of gaseous static azulene in ambient air from Fig. 4. Blue traces: IBBCEAS spectra from Fig. 4 corrected using CRDS-based evaluation (1)-light blue ($\varepsilon_{(1)}$), and CEAS-based evaluation (2)-dark blue ($\varepsilon_{(2)}$).

Both correction methods, **(1)** and **(2)** (light and dark blue traces in Fig. 6 respectively), produce very similar spectra with lower absorption coefficients than the uncorrected IBBCEAS spectrum in Fig. 4, and in accordance with expectation: $\varepsilon_{(1)} \approx \varepsilon_{(2)} < \varepsilon$. The good agreement between $\varepsilon_{(1)}$ and $\varepsilon_{(2)}$ indicates that the light source did not show severe light intensity variations between the CRD measurement without a sample (Fig. 3) and the gated IBBCEAS measurement. To test this aspect further, deliberate numerical variations of up to 20% were introduced in $A_{t=0}$ before the application of the numerical procedure, which led to offsets between $\varepsilon_{(1)}$ and $\varepsilon_{(2)}$ that were of the same percentage order as the fluctuation that was introduced. This shows that the agreement between $\varepsilon_{(1)}$ and $\varepsilon_{(2)}$ is a relative measure of the light source stability. The corrected IBBCEAS spectra in Fig. 6 is approximately 30% lower than the CRD spectrum (see Fig. 4). This approximately constant difference between the spectra (factor 1.3) is attributed to a smaller azulene concentration in the cavity during the IBBCEAS measurement in comparison to the CRDS measurement, due to a time delay of more than 16 min between measurements. It should be noted that the spectrum $\varepsilon_{(2)}(\lambda)$ exhibits somewhat more noise than $\varepsilon_{(1)}(\lambda)$. This is a consequence of the level of noise in the $\tau_0(\lambda)$ spectrum which leads to increased noise in the calculated $\varepsilon_{(2)}(\lambda)$. This is in contrast to $\varepsilon_{(1)}(\lambda)$ which is determined from the lower noise integrated cavity output.

In summary, for gated pulsed IBBCEAS the delay time of the measurement window should be as short as possible to avoid overestimation of the measured absorption. If a CRDS spectrum of the empty cavity is known, the systematic overestimate of the absorption in pulsed IBBCEAS, arising from the gating, can be corrected through a numerical approach. The correction can be

Optics EXPRESS

used to assess the stability of the light source under given experimental conditions. In contrast to gated pulsed IBBCEAS, the intensity-*independent* nature of CRDS does not exhibit this bias, however, with the current approach the CRD measurement times are significantly longer than those for IBBCEAS. Even though broadband pulsed CRDS can be assumed to deliver unbiased absorption data, IBBCEAS (and subsequent correction) eliminates the need for more time-consuming ring-down measurements for each sample.

3.3. Other general features

The emission from the LIP is not only based on a thermal continuum spectrum, which depends on the temperature of the plasma, but it is also characterised by a number of time-dependent atomic emission lines, which are due to the recombination of electrons as the plasma expands (see Section 3.1). The recombination lines are superimposed on the thermal background and their influence on the measurement is determined by the lifetime of the corresponding states (i.e. the allowedness of the transitions involved). Emission lines are also present in the spectrum of the light leaking from the cavity and can lead to some distortions of the measured absorption spectra, which ought to be recognized. This is evident in Fig. 4 at around 616 nm where a long-lived oxygen emission is located [14] (cf. Fig. 3). In principle, the influence of emission lines may be experimentally reduced by choosing a carrier gas with minimal emission in the spectral region of interest, e.g. by using helium as carrier gas in a flow cell setup.

In comparison to the previous work with a confocal cavity and a fs-Nd:glass laser (integration time of 180 ms, SNR = 30) [2], the combination of a near-concentric cavity with a ns-pulsed laser yielded a factor of ~ 3.5 increase in the SNR with a significantly shorter integration time (i.e. 4.5 ms, SNR = 104). This increased SNR is due to the significantly brighter LIP formed by the ns-pulsed laser. This increased SNR in the concentric cavity case is possible despite the factor of 2 increase in mirror separation (cavity length) resulting in a factor of 4 decrease in the light collection efficiency, η, as described by Eq. (4), where D and L are the mirror diameter and cavity length, respectively.

$$\eta = \frac{1}{2}\left(\frac{D}{L}\right)^2 \tag{4}$$

The loss of light due to this decrease in η is offset by the increase in effective path length of the cavity and the significantly brighter LIP. The concentric cavity geometry also has the benefit of increasing the distance of the cavity mirrors from the LIP, which reduces potential exposure of the mirror coatings to any highly reactive (hazardous) species (e.g. ions / radicals) also generated by the plasma and therefore minimizing reflectivity degradation over time.

4. Conclusion

The use of nanosecond laser-induced plasmas as intra-cavity light sources for cavity-enhanced absorption measurements has been demonstrated in a near-concentric cavity. The significant increase in brightness of the nanosecond-LIP provides a marked increase in the SNR when compared to previous absorption studies which utilised an LIP generated by a femtosecond laser pulse. Based on the absorption of gaseous azulene it was demonstrated that both broadband intensity-dependent (IBBCEAS), and time-dependent (CRDS), measurement schemes can be implemented with the LIP approach. The IBBCEAS and CRDS implementations were compared. While gated IBBCEAS has a better time resolution and appears to deliver larger achievable SNR, CRDS enables the calibration of the effective cavity mirror reflectivites, thus facilitating absolute absorption measurements with IBBCEAS. Moreover, in pulsed gated IBBCEAS the absorption is in principle always over-estimated and needs to be corrected numerically, which was illustrated here. The correction can be used to estimate the stability of the light source; in the present case

Optics EXPRESS

the time-averaged LIP. Thus a combination of both implementations (IBBCEAS and CRDS) make LIP based cavity absorption measurements a useful alternative to other methodologies.

Funding

Science Foundation Ireland (11/RFP.1/PHY/3233).

Acknowledgments

The authors would like to thank Prof. J. Orphal (Karlsruhe Institute of Technology, Institute of Meteorology and Climate Research, Germany) for the loan of a fast gated CCD camera, and Mr J. Sheehan (Physics Department, UCC) for his excellent technical assistance.

Disclosures

The authors declare no conflicts of interest.

References

1. S. E. Fiedler, A. Hese, and A. A. Ruth, "Incoherent broad-band cavity-enhanced absorption spectroscopy," Chem. Phys. Lett. **371**(3-4), 284–294 (2003).
2. A. A. Ruth, S. Dixneuf, and J. Orphal, "Laser-induced plasmas in ambient air for incoherent broadband cavity-enhanced absorption spectroscopy," Opt. Express **23**(5), 6092–6101 (2015).
3. A. Czyzewski, S. Chudzyński, K. Ernst, G. Karasiński, Ł. Kilianek, A. Pietruczuk, W. Skubiszak, T. Stacewicz, K. Stelmaszczyk, B. Koch, and P. Rairoux, "Cavity ring-down spectrography," Opt. Commun. **191**(3-6), 271–275 (2001).
4. D. S. Venables, T. Gherman, J. Orphal, J. C. Wenger, and A. A. Ruth, "High sensitivity in situ monitoring of NO_3 in an atmospheric simulation chamber using incoherent broadband cavity-enhanced absorption spectroscopy," Environ. Sci. Technol. **40**(21), 6758–6763 (2006).
5. J. M. Langridge, S. M. Ball, and R. L. Jones, "A compact broadband cavity enhanced absorption spectrometer for detection of atmospheric NO_2 using light emitting diodes," Analyst **131**(8), 916–922 (2006).
6. N. Jordan, C. Z. Ye, S. Ghosh, R. A. Washenfelder, S. S. Brown, and H. D. Osthoff, "A broadband cavity-enhanced spectrometer for atmospheric trace gas measurements and rayleigh scattering cross sections in the cyan region (470–540 nm)," Atmos. Meas. Tech. **12**(2), 1277–1293 (2019).
7. R. A. Washenfelder, A. O. Langford, H. Fuchs, and S. S. Brown, "Measurement of glyoxal using an incoherent broadband cavity enhanced absorption spectrometer," Atmos. Chem. Phys. **8**(24), 7779–7793 (2008).
8. G. Schmidl, W. Paa, W. Triebel, S. Schippel, and H. Heyer, "Spectrally resolved cavity ring down measurement of high reflectivity mirrors using a supercontinuum laser source," Appl. Opt. **48**(35), 6754–6759 (2009).
9. B. P. Keary, "Laser-induced plasmas in air for pulsed broadband cavity-enhanced absorption spectroscopy," Ph.D. thesis, University College Cork, Cork, Ireland (2019).
10. B. P. Keary and A. A. Ruth, "Intra-cavity laser-induced plasmas for enhanced absorption spectroscopy: Intrinsic effects on the cavity output intensity," (2019). To be published.
11. S. E. Fiedler, G. Hoheisel, A. A. Ruth, and A. Hese, "Incoherent broad-band cavity-enhanced absorption spectroscopy of azulene in a supersonic jet," Chem. Phys. Lett. **382**(3-4), 447–453 (2003).
12. A. A. Ruth, E. -K. Kim, and A. Hese, "The $S_0 \rightarrow S_1$ cavity ring-down absorption spectrum of jet-cooled azulene: dependence of internal conversion on the excess energy," Phys. Chem. Chem. Phys. **1**(22), 5121–5128 (1999).
13. A. O'Keefe, "Integrated cavity output analysis of ultra-weak absorption," Chem. Phys. Lett. **293**(5-6), 331–336 (1998).
14. A. Kramida, Yu. Ralchenko, and J. Reader, and NIST ASD Team, NIST Atomic Spectra Database (ver. 5.6.1), [Online]. Available: https://physics.nist.gov/asd. National Institute of Standards and Technology, Gaithersburg, MD. (2018).